Variability of f_oF_2 over Rome and Gibilmanna during three solar cycles (1976-2000)

M. Pietrella,[1] M. Pezzopane,[1] and C. Scotto[1,2]

Received 19 December 2011; revised 27 March 2012; accepted 29 March 2012; published 16 May 2012.

[1] Hourly validated values of the F2-layer critical frequency (f_oF_2) recorded at Rome, Italy (geographic coordinates 41.8°N, 12.5°E; geomagnetic coordinates 42.0°N, 93.8°E), and Gibilmanna, Italy (geographic coordinates 37.6°N, 14.0°E; geomagnetic coordinates 38.1°N, 93.6°E), along with the hourly quiet time reference values of f_oF_2 ($f_oF_{2\mathrm{QTRV}}$) were considered around periods of minimum and maximum solar activity over the years 1976–2000. The f_oF_2 data set was specifically organized in order to obtain an overall trend both for low and high solar activity, and different dispersion indices were used. The results obtained show that (1) at Rome, the f_oF_2 variability is always greater during periods of high solar activity (HSA) in the hourly ranges 00:00–02:00 UT and 20:00–23:00 UT during winter months, and in the hourly ranges 00:00–10:00 UT and 04:00–16:00 UT during equinoctial and summer months respectively; (2) on the whole, around midday, for low solar activity (LSA), the f_oF_2 variability is smaller at the equinoxes than at the solstices; for HSA, it is greater at equinoxes than at solstices; (3) for LSA, at Gibilmanna the f_oF_2 variability is in general larger than at Rome, especially in summer, and it is characterized by a number of relative minimums and maximums greater than those observed at Rome; (4) at Rome, for both LSA and HSA, the passage of solar terminator at sunset significantly affects ionospheric variability in January, April, August, and November, at Gibilmanna in August, September, and November; (5) several variability peaks before sunrise and after sunset are observed in both stations; (6) on a monthly basis, for both LSA and HSA, a semiannual variation of f_oF_2 variability is observed at both Rome and Gibilmanna; and (7) evidence of ionospheric variability at the typical heights of the F region, connected to upward propagating gravity waves triggered by solar terminator, is observed at Rome during some days characterized by HSA in the equinoctial months.

Citation: Pietrella, M., M. Pezzopane, and C. Scotto (2012), Variability of f_oF_2 over Rome and Gibilmanna during three solar cycles (1976-2000), *J. Geophys. Res.*, *117*, A05316, doi:10.1029/2011JA017462.

1. Introduction

[2] Studies of ionospheric variability were carried out in the past using the hourly values of the critical frequencies and the corresponding observed monthly medians of the E region, and of the F1 and F2 ionospheric layers. At mid-latitudes it was found that, compared to the E region and the F1 layer, the F2 layer is by far the most variable [*Rush and Gibbs*, 1973]. Therefore, unlike the monthly median values of f_oE and f_oF_1, the monthly median values of f_oF_2 cannot adequately represent the day-to-day variability of the corresponding layer. As a consequence, median predictions of f_oF_2 would be subject to day-to-day prediction errors in the order of 0.6 to 9.0 MHz when used for radio transmissions on a daily basis [*Rush and Gibbs*, 1973]. From these results, and also considering that the F2 layer is by far the most important ionospheric layer for HF band radio communications, it emerges that F2-layer variability is of much greater importance than that of the E region and F1 layer. For these reasons, over the years many studies have focused on the F2 layer and its variability [e.g., *Elias*, 2009; *Jarvis*, 2009; *Rishbeth et al.*, 2009; *Chen and Liu*, 2010; *David and Sojka*, 2010; *Liu et al.*, 2011; *Somoye et al.*, 2011; *Triskova et al.*, 2011; *Zolotukhina et al.*, 2011].

[3] Several studies have now demonstrated that F2-layer variability occurs over a wide range of time scales, from hours to years, and depends basically on three different physical sources: solar flux changes, geomagnetic activity, and meteorological processes.

[4] The solar source seems to be much more important for f_oF_2 month-to-month and year-to-year variability (i.e., following the 11 year solar cycle). Even though day-to-day variations of the F2-layer height are found to be well correlated with day-to-day variations in solar activity [*Rishbeth*, 1993], the ionospheric variability associated with day-to-day

[1]Istituto Nazionale di Geofisica e Vulcanologia, Rome, Italy.
[2]Also at Doctoral School in Polar Sciences, University of Siena, Siena, Italy.

Corresponding author: M. Pietrella, Istituto Nazionale di Geofisica e Vulcanologia, Via di Vigna Murata 605, Rome I-00143, Italy. (marco.pietrella@ingv.it)

0148-0227/12/2011JA017462

solar flux changes is estimated in terms of the normalized standard deviation to be about 3% and hence it is small when compared with that due to meteorological influences (18%) [*Forbes et al.*, 2000].

[5] Very marked ionospheric variability is observed during significant disturbances affecting the Earth's magnetic field and related to geomagnetic storms. In these cases, significant changes of the electron density can alter day-to-day F2-layer variability [e.g., *Prolss*, 1995; *Prölss*, 1997; *Fuller-Rowell et al.*, 1997; *Buonsanto*, 1999].

[6] Equally important are the "meteorological effects," i.e., those dynamic phenomena propagating from the lower atmosphere (such as atmospheric tides, internal gravity waves, planetary waves) up to ionospheric heights, and that are in part responsible for the ionospheric variability observed in the F2 layer [*Kazimirovsky*, 2002, and reference therein]. Other studies, aimed to determine which fraction of the observed F2-layer variability could be attributed to the different causes, showed that the meteorological sources are comparable with the geomagnetic sources [*Rishbeth and Mendillo*, 2001].

[7] Quantifying to what extent observed F2-layer variability is due to the various sources, is very important because this would permit a much more detailed understanding of the ionosphere. This knowledge would be fundamental for developing and improving statistical models of ionospheric variability valuable to assist HF operators in planning and maintaining efficient management of HF radio communications.

[8] In the past, the study of ionospheric variability was performed using different dispersion indices. The f_oF_2 monthly median values are usually considered as representative of a quiet state of the ionosphere [*Cander and Mihajlovic*, 1998], and for this reason some studies regarding ionospheric variability were conducted by analyzing the statistical distributions of dispersion indices based on the monthly median values [*Kouris et al.*, 1998, 1999]. In addition to the monthly medians, the lower and upper deciles can also be regarded as a useful tool in providing a standard and statistical description of the ionosphere [*Wilkinson*, 2004]. The fractional decile deviations from the monthly medians for different seasons, geographical latitudes, and range of solar activity, were used to model day-to-day f_oF_2 and *M*(3000)F2 variations [*Davis and Groome*, 1964]. This statistical model of ionospheric variability was implemented by the International Communication Union (ITU) [*ITU*, 1997] to provide an estimation of diurnal MUF variability as a guideline for the choice of the maximum usable frequencies for use in radio communications.

[9] More recently, a day-to-day MUF variability has been investigated using decile factors calculated with data from more than a hundred ionospheric stations spread worldwide, and compared with those of the ITU, currently used by the international radio community [*Fotiadis et al.*, 2004]. It should be noted that monthly medians and deciles have their limitations. In fact, it is not easy to define a parameter that accurately represents a "quiet" ionosphere. The f_oF_2 monthly median values give rise to many artificial effects [*Kozin et al.*, 1995] and can be inadequate to describe a "quiet" ionosphere. Alternative quiet time reference values are required [*Wrenn et al.*, 1987]. Moreover, *Fox and Wilkinson* [1988] found that while the decile factors were effective at times, they often significantly under- or over-estimate the observed variability.

[10] From these considerations, and in order to identify a dispersion index that is able to objectively quantify ionospheric variability, the authors deduced that it is of crucial importance to define the representative parameters of a "quiet" ionosphere.

[11] A tool for assessing dispersion of measurements over a given period is standard deviation. Due to natural fluctuations of the ionospheric reflector, f_oF_2 measurements vary. Many f_oF_2 measurements close to the average value indicate a very small variability and hence such measurements can be considered "representative" of a quiet period. Therefore, standard deviation seems to be appropriate to identify periods in which the observed variations of f_oF_2 are not significant. For these reasons, this parameter was widely used to investigate ionospheric variability [*Forbes et al.*, 2000; *Rishbeth and Mendillo*, 2001; *Bilitza et al.*, 2004; *Akala et al.*, 2010].

[12] This work represents a further contribution to this approach, and describes a study of f_oF_2 variability over Rome, Italy (41.8°N, 12.5°E), and Gibilmanna, Italy (37.6°N, 14.0°E), for low solar activity (LSA) and high solar activity (HSA) over three solar cycles. The coordinate written above place both stations within the meridian following the Greenwich meridian. With this in mind, even if this investigation was conducted using the hourly values of f_oF_2 taken in universal time (UT), the results acquired in this study can be thought in terms of local time (LT) adding one hour, being the relationship between UT and LT at both stations given by LT = UT + 1.

[13] Section 2 describes the data sets considered, and their corresponding organization. Section 3 defines the different dispersion indices considered in order to perform the analysis, and illustrates the related results, which are discussed in section 4. Concluding remarks and possible future developments are summarized in section 5.

2. Data Sets

[14] In order to perform the analysis described in this paper, two different data sets were considered. The first includes the f_oF_2 hourly validated values recorded at the ionospheric stations of Rome and Gibilmanna over three solar cycles (January 1976 - December 2000). The second includes the hourly quiet time reference values (f_oF_{2QTRV}), calculated for the same period of time, following the procedure proposed by *Wrenn et al.* [1987] and described in detail by *Pietrella and Perrone* [2008].

[15] With regard to the f_oF_2 validated values, they were interpreted according to the International Union of Radio Science (URSI) standard [*Wakai et al.*, 1987], and all the corresponding numerical values were considered independently of the presence of qualifying and descriptive letters. These validated data were downloaded from the electronic Space Weather upper atmosphere database (eSWua; http://www.eswua.ingv.it/) [*Romano et al.*, 2008].

[16] The procedure followed for the arrangement of both data sets consists of two fundamental steps: (1) The months of lowest and highest solar activity were identified for each of the three solar cycles considered (see Table 1), and (2) the six months prior and following each month identified in

Table 1. Months of Lowest and Highest Solar Activity for Solar Cycles 21, 22, and 23, With Corresponding Value of the Solar Index R_{12}

	Lowest Solar Activity	Highest Solar Activity
Solar cycle 21	Jun 1976 (R_{12} = 12.2)	Dec 1979 (R_{12} = 164.5)
Solar cycle 22	Sep 1986 (R_{12} = 12.3)	Jul 1989 (R_{12} = 158.5)
Solar cycle 23	May 1996 (R_{12} = 8.0)	Apr 2000 (R_{12} = 120.8)

step 1 were considered, and consequently six groups of 13 months, three for LSA and three for HSA, were formed (see Table 2).

[17] As in the case of HSA solar cycle 23 has a much lower maximum solar index (R_{12} around 120) than the solar cycles 21 and 22 that present very close maximum solar indices (R_{12} around 160), the hourly mean values of f_oF_2 were calculated for each solar cycle considering the months characterized by HSA (Table 2) and then plotted to have a confirmation of the F2 layer saturation effect. As can be seen in Figure 2, f_oF_2 values from solar cycle 23 are not much different from those of solar cycle 21 and 22, except for January, February, October, November, and December that present significantly lower values than those of the solar cycle 21 and 22. This means that the saturation effect for these months is not verified; that is why these months (footnoted in Table 2) were excluded from the analysis concerning HSA data set.

[18] With regard to Gibilmanna, only data for LSA were considered because of an important lack of HSA data.

[19] Given the data set arrangement shown in Table 2, the f_oF_2 hourly validated values for a given month were grouped to obtain two different data sets: one for LSA and the other for HSA. These two data sets were then binned in terms of single hour, so that each bin includes hourly time series of f_oF_2, one for LSA and the other one for HSA. At the end of this procedure, 24 data sets for each month both for LSA and HSA were created (see Figure 1).

[20] Similarly, 24 data sets for LSA and 24 data sets for HSA were obtained for each month by taking into account the corresponding f_oF_{2QTRV} hourly values.

Table 2. Six Groups of 13 months, Three for Low Solar Activity and Three for High Solar Activity, Each of Which Is Centered on the Corresponding Month of Lowest and Highest Solar Activity Shown in Table 1

Low Solar Activity			High Solar Activity		
Group 1	Group 2	Group 3	Group 1	Group 2	Group 3
Dec 1975	Mar 1986	Nov 1995	Jun 1979	Jan 1989	Oct 1999[a]
Jan 1976	Apr 1986	Dec 1995	Jul 1979	Feb 1989	Nov 1999[a]
Feb 1976	May 1986	Jan 1996	Aug 1979	Mar 1989	Dec 1999[a]
Mar 1976	Jun 1986	Feb 1996	Sep 1979	Apr 1989	Jan 2000[a]
Apr 1976	Jul 1986	Mar 1996	Oct 1979	May 1989	Feb 2000[a]
May 1976	Aug 1986	Apr 1996	Nov 1979	Jun 1989	Mar 2000
Jun 1976	Sep 1986	May 1996	Dec 1979	Jul 1989	Apr 2000
Jul 1976	Oct 1986	Jun 1996	Jan 1980	Aug 1989	May 2000
Aug 1976	Nov 1986	Jul 1996	Feb 1980	Sep 1989	Jun 2000
Sep 1976	Dec 1986	Aug 1996	Mar 1980	Oct 1989	Jul 2000
Oct 1976	Jan 1987	Sep 1996	Apr 1980	Nov 1989	Aug 2000
Nov 1976	Feb 1987	Oct 1996	May 1980	Dec 1989	Sep 2000
Dec 1976	Mar 1987	Nov 1996	Jun 1980	Jan 1990	Oct 2000[a]

[a]Months that were excluded from the analysis because the saturation effect is not proved.

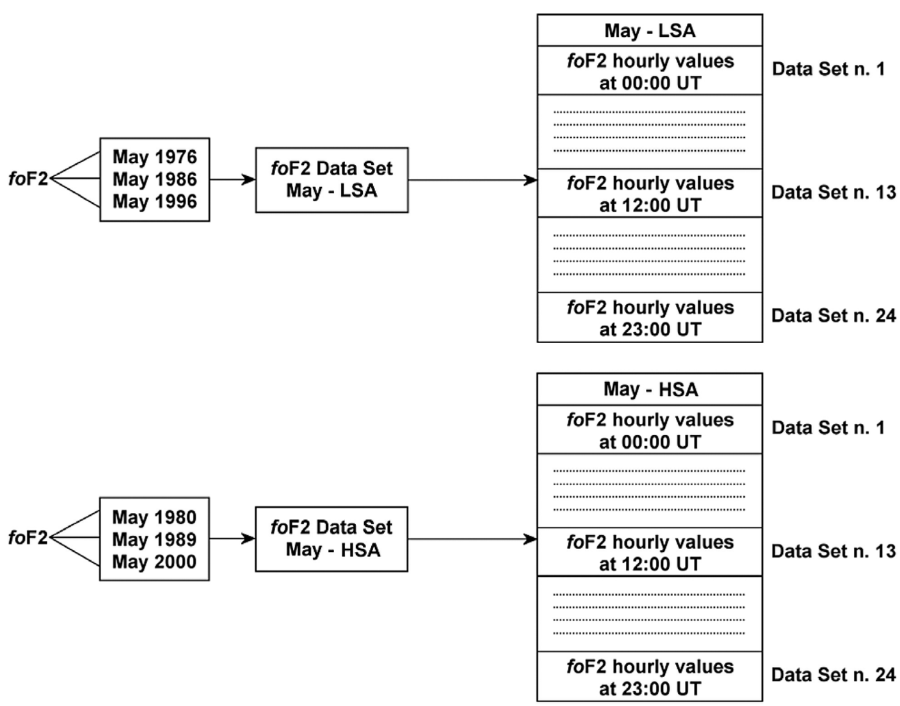

Figure 1. Scheme illustrating the procedure by which, according to the grouping shown by Table 2, 24 data sets are created for both low solar activity (LSA) and high solar activity (HSA) for each month considered (the figure refers to May).

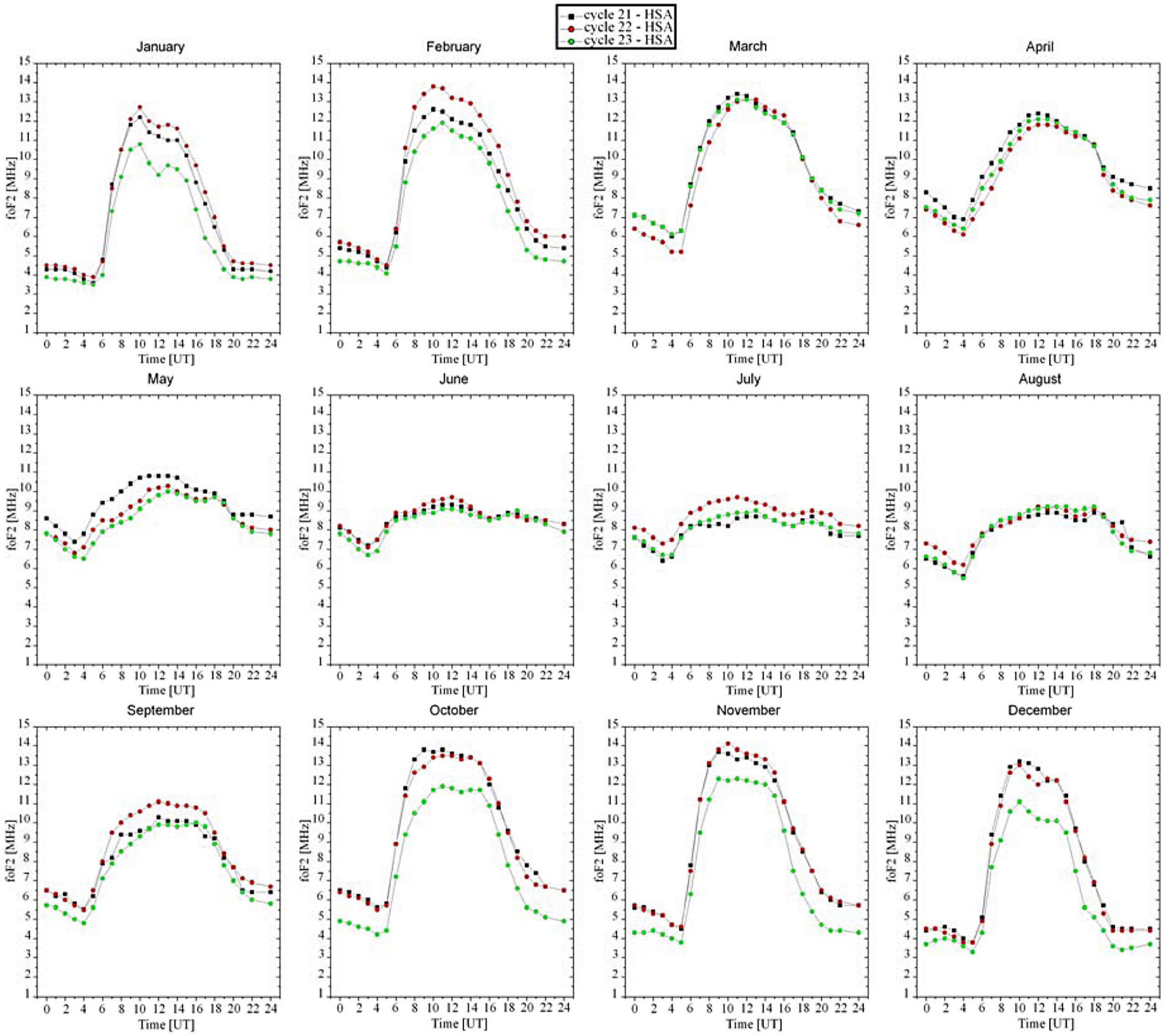

Figure 2. Hourly mean values of f_oF_2 calculated for those months characterized by HSA (according to Table 2), for solar cycle 21 (black dots), 22 (red dots), and 23 (green dots).

[21] From each hourly data set generated following the procedure just described, the hourly mean of f_oF_2 were calculated. Figure 3 shows the diurnal plots of the f_oF_2 mean values on monthly scales at Rome in case of HSA and at Rome and Gibilmanna for LSA.

3. Dispersion Indices and Results

[22] Based on the two different data sets introduced in section 2 and on the corresponding organization, two different dispersion indices, for a given month and hour, were calculated. The first is

$$\sigma_{\overline{fo\,\mathrm{F2}}}(\text{month, hour}) = \sqrt{\frac{\sum_{i=1}^{N}\left(fo\,\mathrm{F2}(\text{year, month, day, hour})_i - \overline{fo\,\mathrm{F2}}(\text{month, hour})\right)^2}{N}}, \quad (1)$$

where

$$\overline{fo\,\mathrm{F2}}(\text{month, hour}) = \frac{\sum_{i=1}^{N} fo\,\mathrm{F2}(\text{year, month, day, hour})_i}{N},$$

f_oF_2(year, month, day, hour) is the hourly validated value for a given year, month, day and hour, and N represents the number of days for which an f_oF_2 hourly validated value is available for that month and hour (for example, referring to the May–HSA data set of Figure 1, if all the data were available N would be equal to 93). The second is

$$\sigma_{foF2_{QTRV}}(\text{month, hour}) = \sqrt{\frac{\sum_{i=1}^{N}\left(fo\,\mathrm{F2}(\text{year, month, day, hour})_i - fo\mathrm{F2_{QTRV}}(\text{year, month, day, hour})_i\right)^2}{N}}, \quad (2)$$

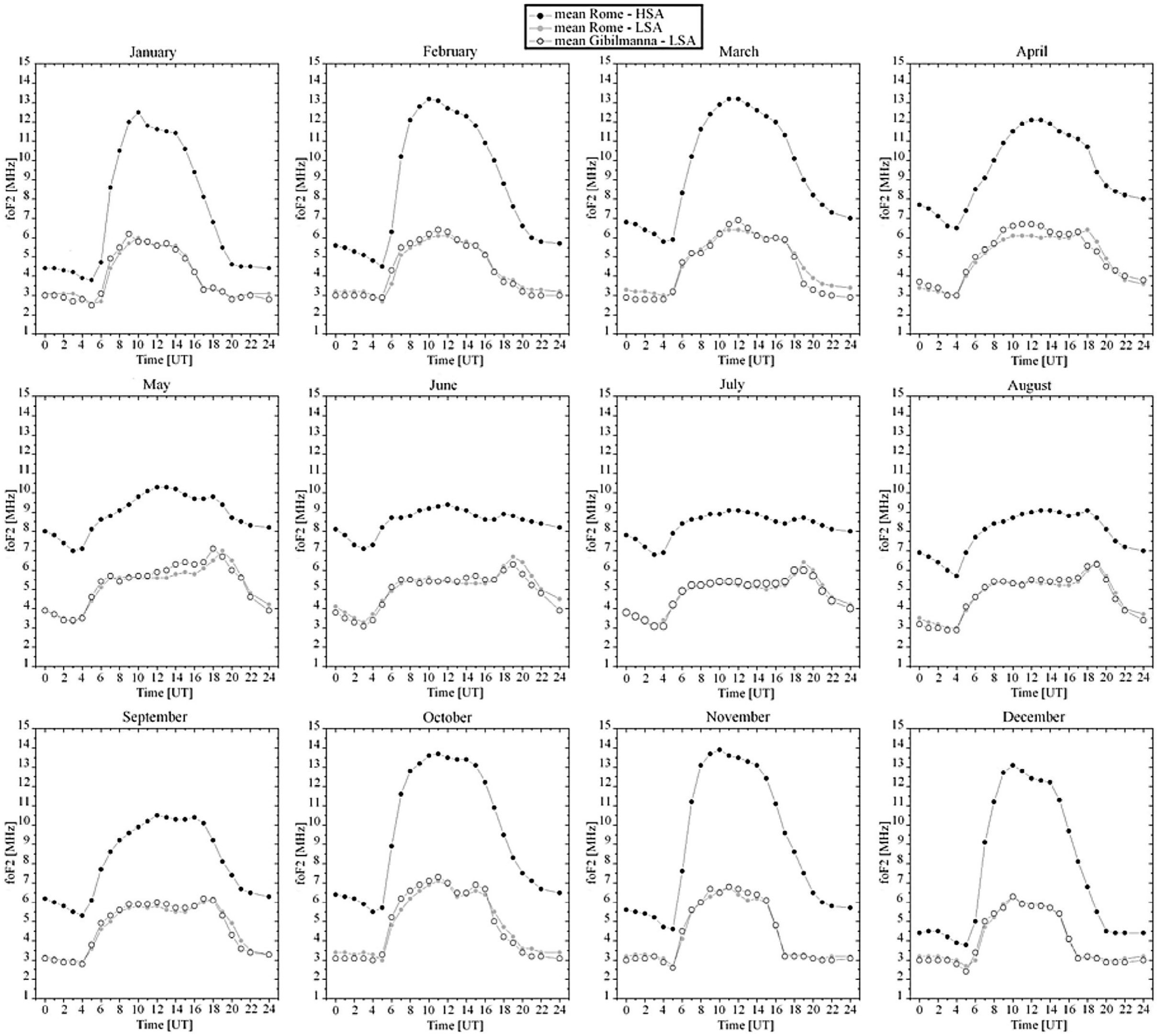

Figure 3. Diurnal variations of the f_oF_2 mean values for all the months during HSA at Rome (black dots) and LSA at Rome (gray dots) and Gibilmanna (white open dots).

where $f_oF_{2\mathrm{QTRV}}$(year, month, day, hour) is the quiet time reference value calculated at the same epoch of the considered hourly validated value. Hence, 24 hourly values were calculated for each month for both equations (1) and (2).

[23] Equation (1) represents the absolute standard deviation based on the f_oF_2 hourly validated values and the corresponding average, while equation (2) is a new dispersion index introduced by comparing the f_oF_2 hourly validated values with the corresponding $f_oF_{2\mathrm{QTRV}}$ values calculated at the same epochs, according to the procedure described by *Pietrella and Perrone* [2008]. The diurnal trends of the ionospheric variability at Rome and Gibilmanna expressed by the dispersion indices (1) and (2) are shown in Figure 4 and Figure 5 respectively, for each month, for LSA for both stations, and for HSA only for Rome.

[24] In order to investigate f_oF_2 variability on a monthly basis, the following monthly averages

$$\bar{\sigma}_{\overline{fo\,\mathrm{F2}}}(\mathrm{month}) = \frac{\sum_{\mathrm{hour}=0}^{\mathrm{hour}=23} \sigma_{\overline{fo\,\mathrm{F2}}}(\mathrm{month, hour})}{24}, \qquad (3)$$

and

$$\bar{\sigma}_{fo\mathrm{F2}_{\mathrm{QTRV}}}(\mathrm{month}) = \frac{\sum_{\mathrm{hour}=0}^{\mathrm{hour}=23} \sigma_{fo\mathrm{F2}_{\mathrm{QTRV}}}(\mathrm{month, hour})}{24}, \qquad (4)$$

of the 24 corresponding hourly values of equations (1) and (2) were calculated, respectively. Figure 6 shows the trend of equations (3) and (4) for LSA, at Rome and at Gibilmanna, and for HSA at Rome.

[25] In order to widen this investigation, according to *Bilitza et al.* [2004] and *Akala et al.* [2010], the following relative standard deviation ($\sigma_{\mathrm{r.s.d.}}$) was also calculated:

$$\sigma_{r.s.d.}(\mathrm{month, hour})[\%] = \frac{\sigma_{\overline{fo\,\mathrm{F2}}}(\mathrm{month, hour})}{\overline{fo\,\mathrm{F2}}(\mathrm{month, hour})} \cdot 100 \qquad (5)$$

In addition, starting from the relative standard deviation, the following monthly averages were calculated:

$$\bar{\sigma}_{r.s.d.}(\mathrm{month})[\%] = \frac{\sum_{\mathrm{hour}=0}^{\mathrm{hour}=23} \sigma_{r.s.d.}(\mathrm{month, hour})[\%]}{24} \qquad (6)$$

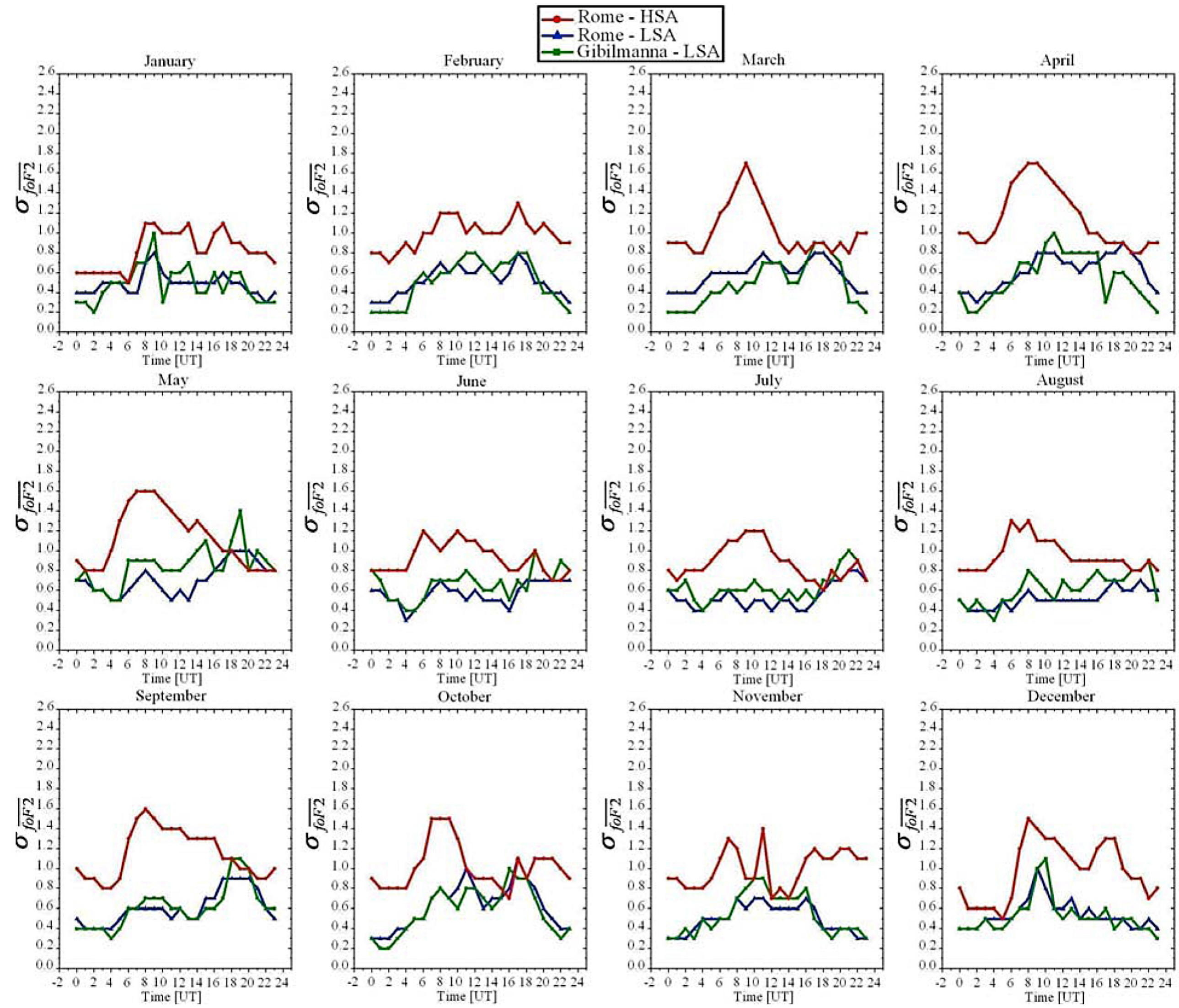

Figure 4. Diurnal trends of ionospheric variability expressed by the absolute standard deviation (1) for each month, for LSA at Rome (blue curve) and at Gibilmanna (green curve) and for HSA at Rome (red curve).

and a new index, similar to those defined in equations (3) and (4), was defined to explore again f_oF_2 variability on a monthly basis.

[26] Figure 7 and Figure 8 depict, for each month, the diurnal plots of the ionospheric variability at Rome and Gibilmanna expressed by the dispersion indices (5) and (6) respectively, for LSA for both stations, and for HSA only for Rome.

[27] In order to look for further additional features characterizing f_oF_2 variability, the following indices were also introduced:

$$\delta_{fo\,\mathrm{F2}}(\text{year, month, day, hour}) = \frac{fo\mathrm{F2}^2(\text{year, month, day, hour}) - \overline{fo\,\mathrm{F2}}^2(\text{year, month, hour})}{\overline{fo\,\mathrm{F2}}^2(\text{year, month, hour})}, \tag{7}$$

where

$$\overline{fo\,\mathrm{F2}}(\text{year, month, hour}) = \frac{\sum_{i=1}^{n} fo\,\mathrm{F2}(\text{year, month, day, hour})_i}{n},$$

and n represents the number of days for which an f_oF_2 hourly validated value is available for that year, month and hour, and

$$\delta_{fo\mathrm{F2}_{\mathrm{QTRV}}}(\text{year, month, day, hour}) = \frac{fo\mathrm{F2}^2(\text{year, month, day, hour}) - fo\mathrm{F2}^2_{\mathrm{QTRV}}(\text{year, month, day, hour})}{fo\mathrm{F2}^2_{\mathrm{QTRV}}(\text{year, month, day, hour})}. \tag{8}$$

The daily trends according to equations (7) and (8) obtained for Rome, for LSA in 1996, and for HSA in

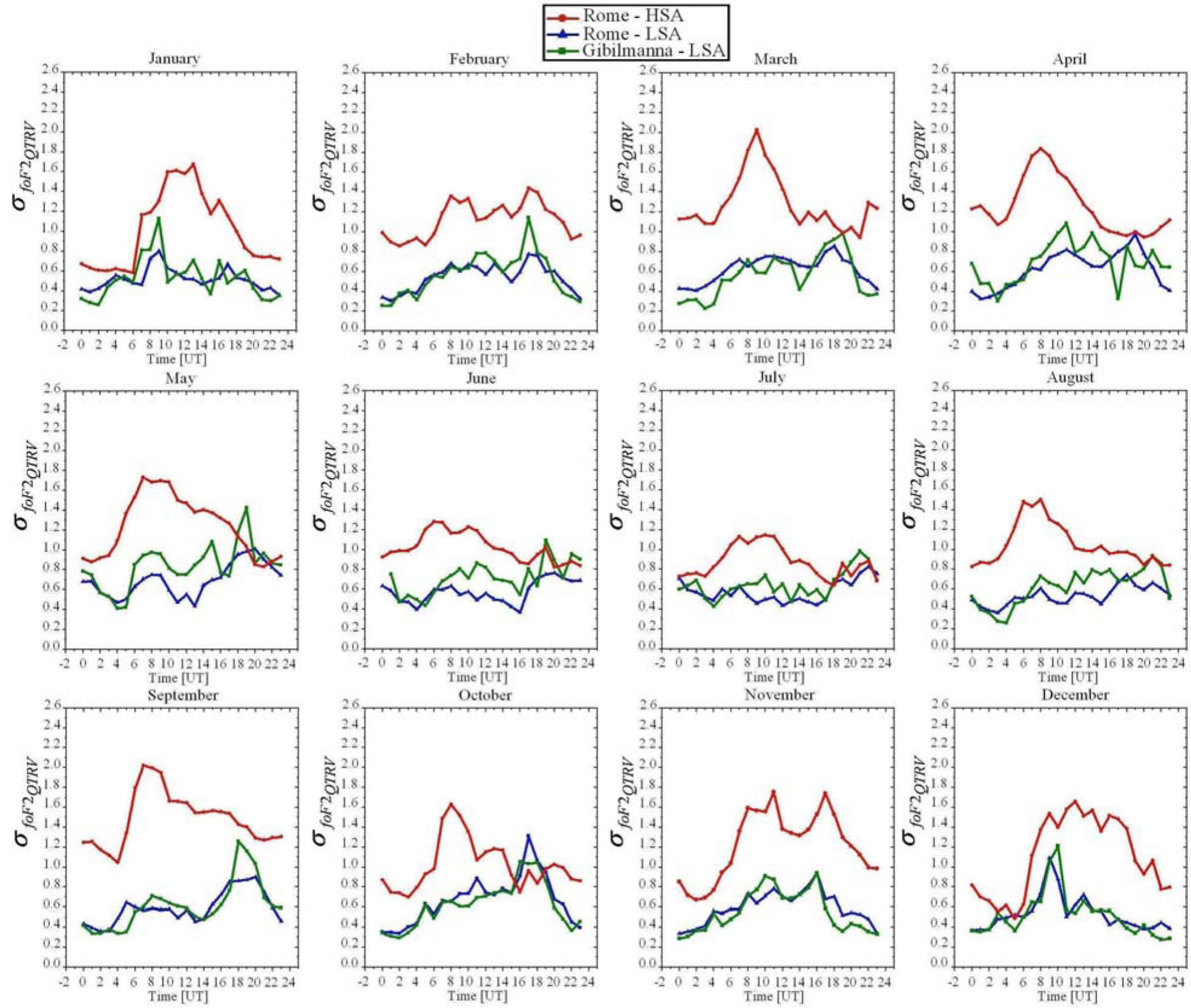

Figure 5. Diurnal trends of ionospheric variability expressed by the dispersion index (2) for each month, for LSA at Rome (blue curve) and at Gibilmanna (green curve) and for HSA at Rome (red curve).

1989 and 2000, are shown respectively in Figure 9, Figure 10, and Figure 11.

4. Discussion

[28] Figure 3 shows the diurnal plots of the mean values of f_oF_2 on monthly scale for HSA (Rome), and LSA (Rome and Gibilmanna). All the plots are characterized by the same diurnal features: high mean values of f_oF_2 during the daytime, with a typical maximum around midday, and low mean values during the nighttime. In particular, a post midnight minimum is observed at 05:00 UT, 04:00 UT, and 03:00 UT in winter, equinoctial and summer months respectively. The maximum around midday clearly emerges in winter and equinoctial months, but is less distinguishable in summer months where a post midnight maximum is detected at 18:00 UT. In case of LSA very similar trends are found for all the months.

[29] In order to provide an overall depiction of f_oF_2 variability in terms of high and low solar activity, the data were organized in a particular way, as shown in section 2. Moreover, besides taking into account the absolute standard deviation (equation (1)), this work also defined a new dispersion index (equation (2)) based on the $f_oF_{2\mathrm{QTRV}}$ values. The trends shown by Figure 4 and Figure 5 clearly highlight that these two indices provide a very similar depiction of ionospheric variability, and hence they can be considered equivalent. Nevertheless, it should be noted that the index (2) derives from the direct comparison of each f_oF_2 measurement validated at a given epoch with the corresponding $f_oF_{2\mathrm{QTRV}}$ value calculated at the same epoch, according to the procedure described by *Pietrella and Perrone* [2008]. With regard to these $f_oF_{2\mathrm{QTRV}}$ values, *Pietrella and Perrone* [2008] demonstrated their reliability by testing their behavior under disturbed ionospheric conditions. For this reason, even though the two indices provide results quantitatively comparable, the authors suggest that to some extent the index (2) can be considered as more reliable than the absolute standard deviation (1).

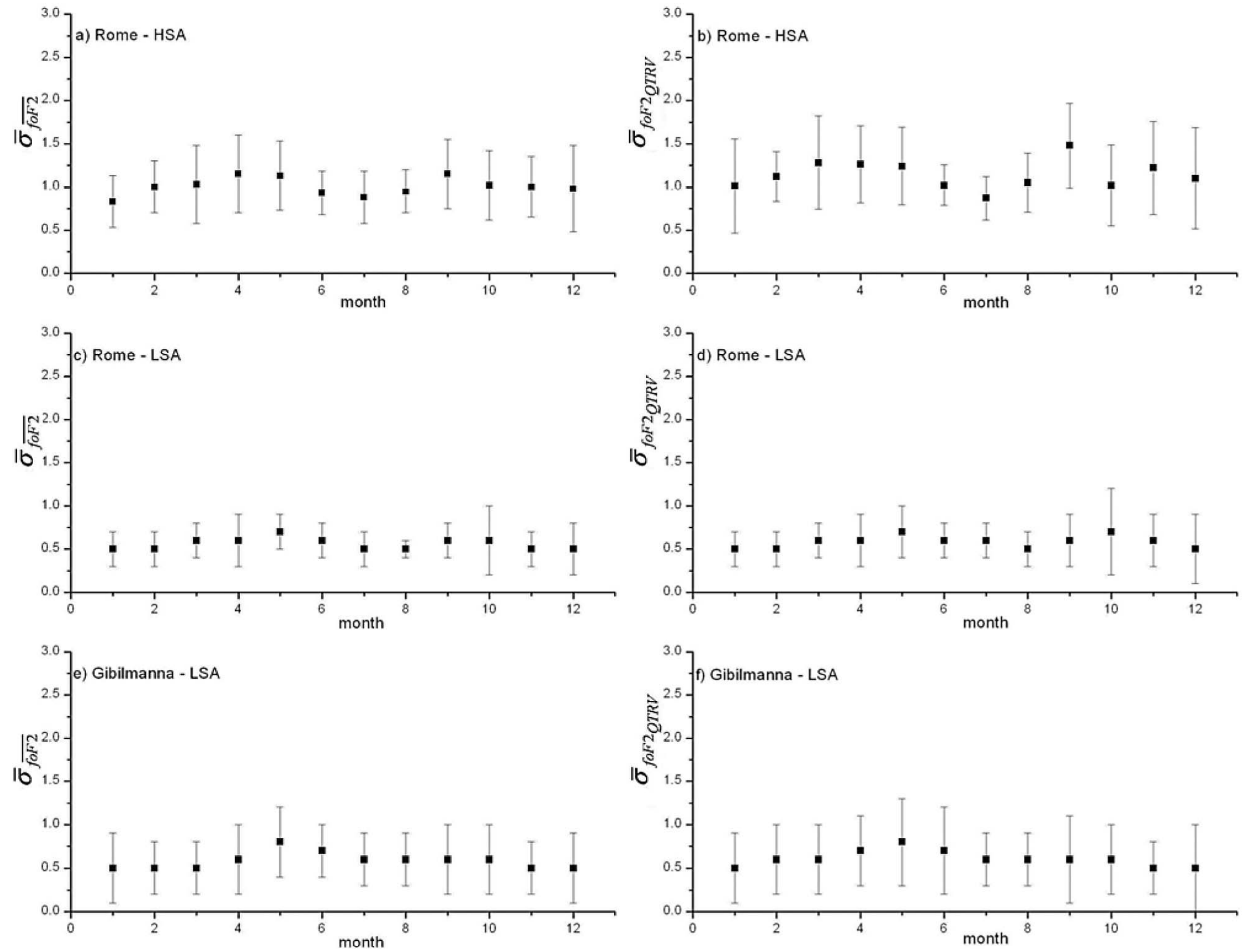

Figure 6. Trend according to (3) at Rome for (a) HSA, (c) LSA, and (e) at Gibilmanna for LSA and according to (4) at Rome for (b) HSA, (d) LSA, and (f) at Gibilmanna for LSA. Error bar of each value is the maximum semidispersion.

[30] Figure 4 and Figure 5 show that at Rome ionospheric variability is always greater for HSA, which agrees with the findings of *Rush and Gibbs* [1973], who established that at midlatitudes the absolute standard deviation is larger at solar maximum than at solar minimum.

[31] The visual inspection of Figure 4 and 7 shows that that absolute and relative standard deviation provide different results. The f_oF_2 variation in terms of solar activity and time of the day fully explains the results of Figure 4. On the other hand, the diurnal variation of f_oF_2, higher at midday than at night, determines a higher percentage ionospheric variability during nighttime (Figure 7) when smaller mean f_oF_2 values are considered. Anyway, the absolute and relative standard deviation provide to some extent the same results. Indeed, a greater ionospheric variability for HSA, but only for certain hours, emerges also from a meticulous analysis of the plot concerning the relative standard deviation; by and large, at Rome, percentage ionospheric variability is in fact always greater for HSA in the hourly ranges 00:00–02:00 UT and 20:00–23:00 UT in winter months, and in the hourly ranges 00:00–10:00 UT and 04:00–16:00 UT in equinoctial and summer months respectively (see red and blue plots of Figure 7).

[32] On the contrary, percentage ionospheric variability is always greater for LSA in the hourly ranges 08:00–16:00 UT and 15:00–21:00 UT in winter and equinoctial months respectively, and in the hourly ranges 00:00–03:00 UT and 17:00–23:00 UT during summer months. These results agree with the outcome of several low latitude investigations [*Bilitza et al.*, 2004; *Ezquer et al.*, 2004; *Akala et al.*, 2010] where it is shown that ionospheric variability increases as solar activity decreases.

[33] From the hourly values of the absolute and relative standard deviation averaged over 5 h from 09:00 to 13:00 UT (not here shown), emerges that for LSA, ionospheric variability is smaller at the equinoxes than at the solstices. On the contrary, for HSA, the variability is on the whole greater at the equinoxes than at the solstices, confirming the findings of *Rishbeth and Mendillo* [2001] and *Ezquer et al.* [2004]. In addition, this seasonal feature does not show any particular asymmetry, which matches the observation of *Liu et al.* [2010], who said that the equinoctial asymmetry in ionospheric plasma density is mainly a low-latitude phenomenon, mostly during LSA. Moreover, the inspection of the absolute and relative standard deviation values around midday provides the same following results: At Rome

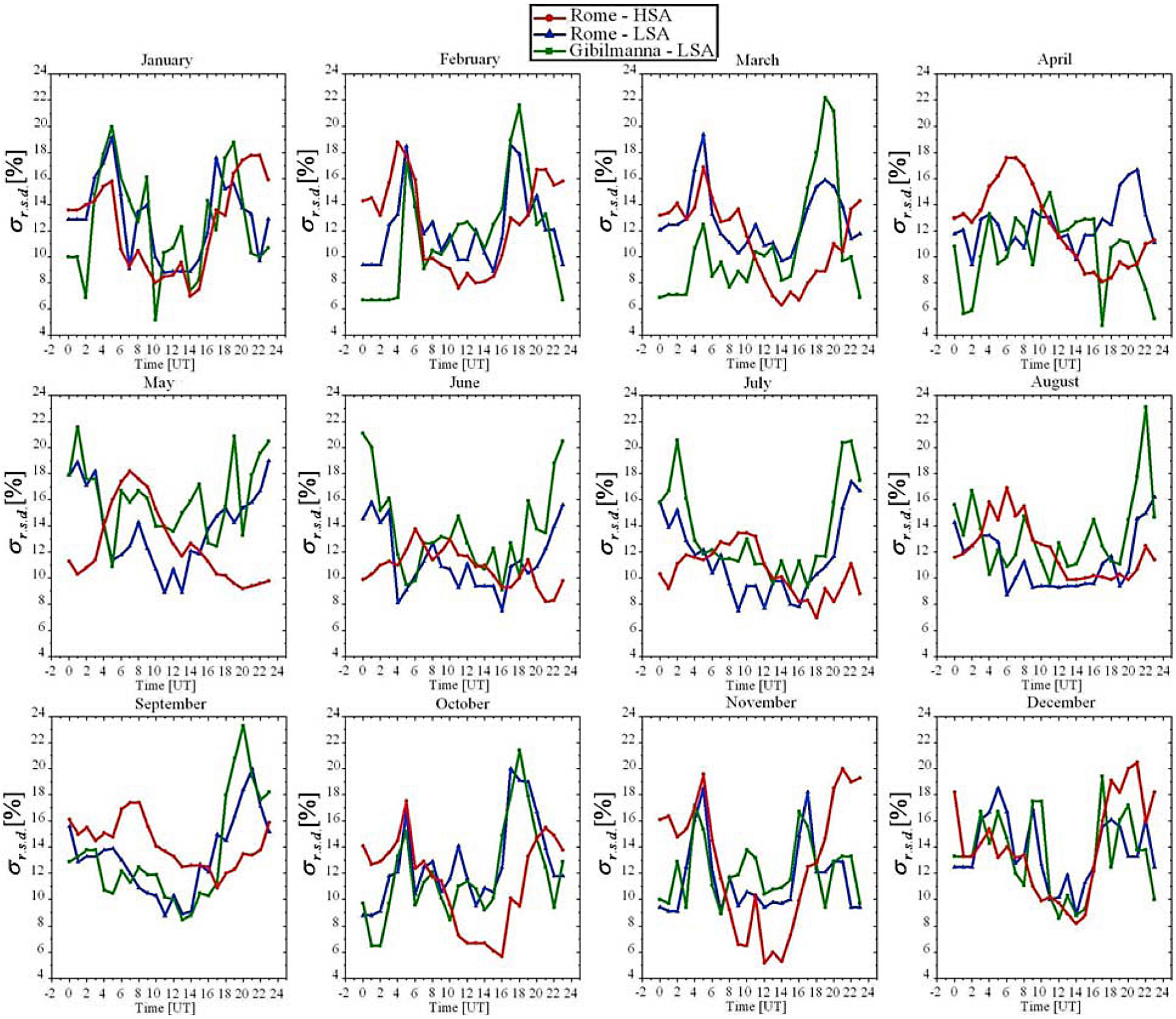

Figure 7. Diurnal trends of ionospheric variability expressed by the relative standard deviation (5) for each month, for LSA at Rome (blue curve) and at Gibilmanna (green curve) and for HSA at Rome (red curve).

ionospheric variability is smaller in case of LSA during summer months; at Gibilmanna ionospheric variability is greater than that in Rome during winter and summer months, and slightly smaller during equinoctial months.

[34] From Figure 4 and Figure 5 it also emerges that for LSA, the variability at Gibilmanna is characterized by a number of relative minimums and maximums greater than those observed at Rome. Although less evident, this feature is also deduced analyzing the trends of the relative standard deviation (see blue and green plots of Figure 7).

[35] Moreover, while a month to month comparison between the diurnal trends of Rome and Gibilmanna does not indicate any particularly noteworthy features in the equinoctial (March, April, September, and October) and winter months (January, February, November, and December), a clearly greater variability during summer months (May, June, July, and August) is observed at Gibilmanna. These results find a confirmation from the examination of the diurnal trends of ionospheric variability expressed by the dispersion index (5).

[36] In fact analyzing meticulously the plots of the relative standard deviation for LSA at Rome and Gibilmanna (blue and green plots of Figure 7), an ionospheric variability greater at Gibilmanna during summer months is generally found in the hourly ranges 00:00–04:00 UT, 06:00–16:00 UT, and 19:00–23:00 UT.

[37] Therefore, it can be argued that Gibilmanna, especially in summer, is more susceptible to variability, with its lower latitude resulting in an ionosphere affected by more numerous dynamic processes.

[38] By and large, the diurnal trends of ionospheric variability obtained for Rome and Gibilmanna (Figures 4, 5, and 7) show the presence of peaks around both sunrise and sunset, probably due to a sudden electron density increase/decrease caused by the turning-on/turning-off of ionizing solar radiation. To verify whether the observed maximums of variability around sunrise/sunset are due to the passage of

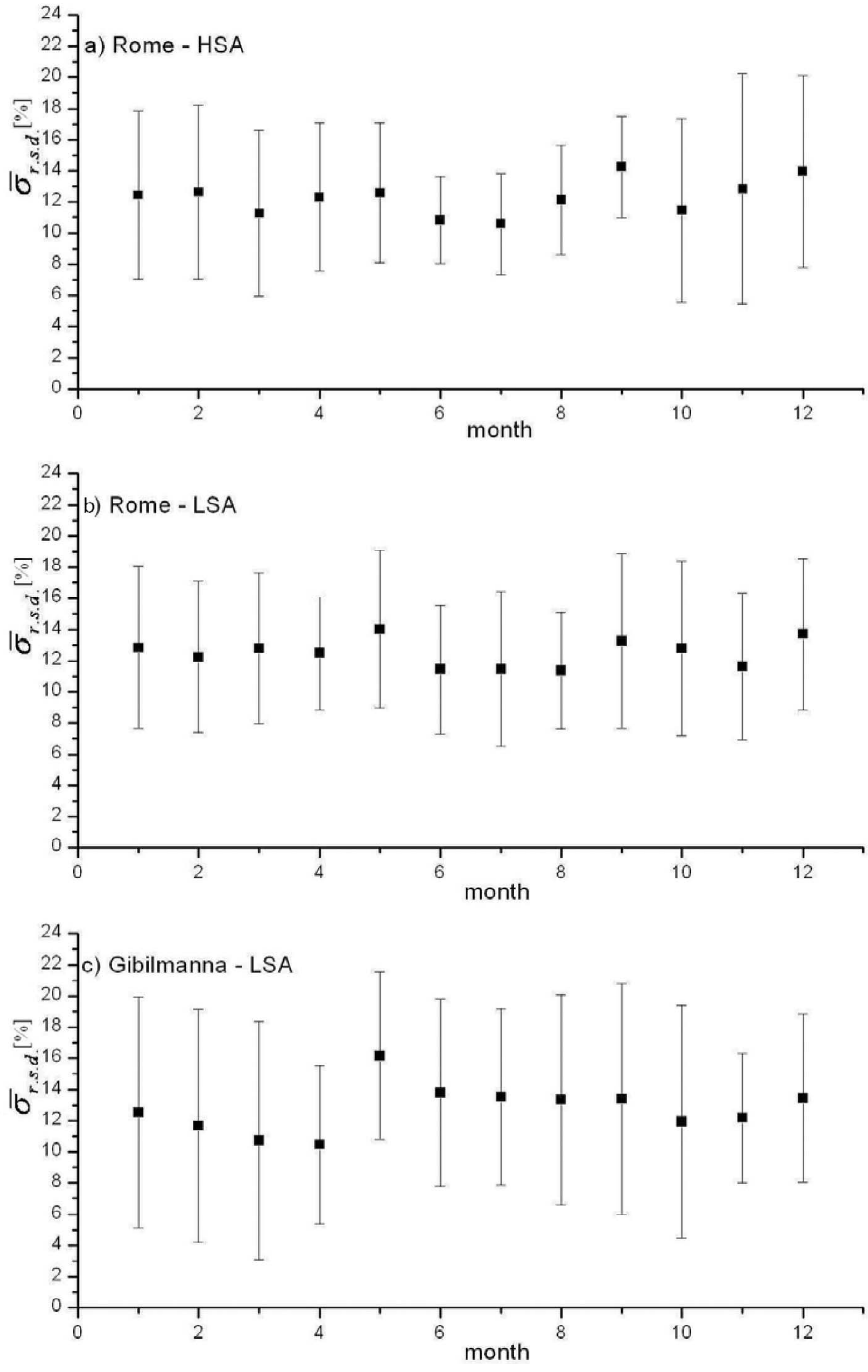

Figure 8. Trend according to (6) at Rome for (a) HSA, (b) LSA, and (c) at Gibilmanna for LSA. Error bar of each value is the maximum semidispersion.

solar terminator, the hourly ranges in which sunrise and sunset occur were calculated for each month at Rome and Gibilmanna taking as reference the year 2011 (see Table 3). The hours which "fall" inside the hourly range delimiting the sunrise/sunset sector, and the number of times (in brackets) for which f_oF_2 measurements occur during nighttime (N_{night}) and during daytime (N_{day}) are also reported in Table 3 for each month.

[39] Ionospheric variability should be mostly affected by the passage of solar terminator when N_{night} and N_{day} are comparable and not in case of $N_{night} \ll N_{day}$ or $N_{day} \ll N_{night}$. The footnoted entries in Table 3 marks the cases for which the passage of solar terminator is expected to affect significantly ionospheric variability under the assumption that is at least $N_{night} \geq 6$ and $N_{day} \geq 6$. To establish whether the peaks of variability observed both with absolute and

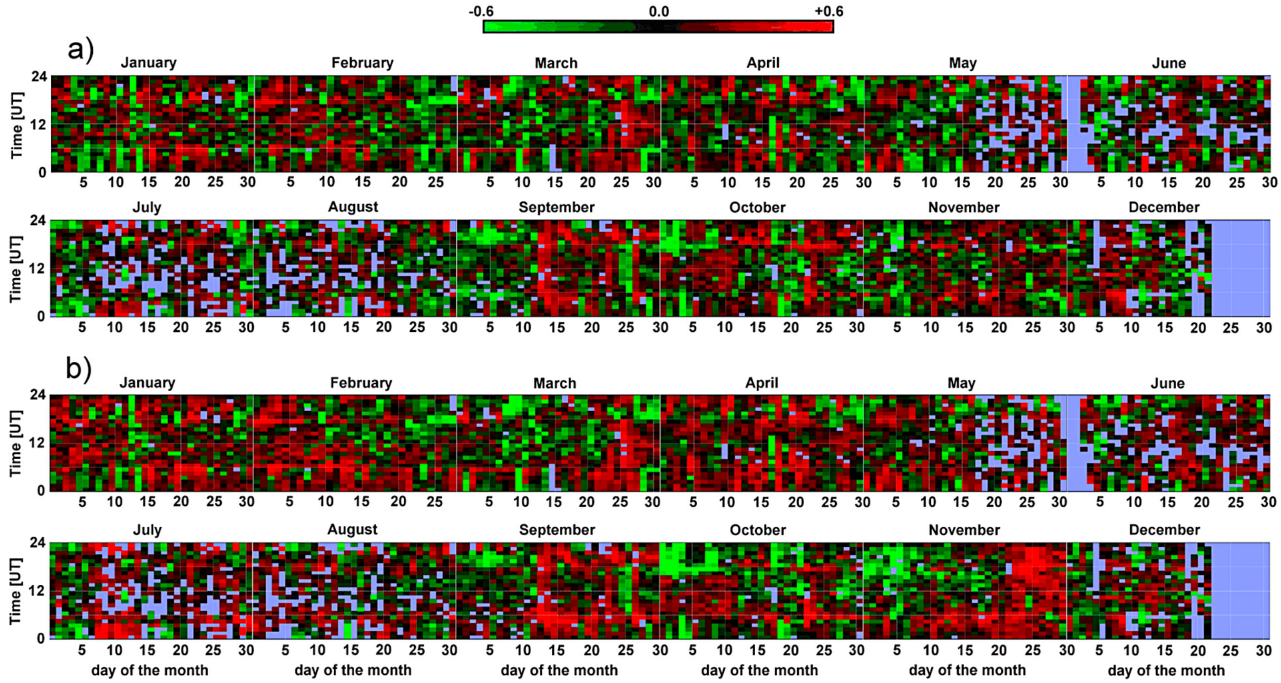

Figure 9. Daily trends obtained for Rome, for LSA (year 1996), according to the index defined by (a) equation (7) and by (b) equation (8). Red and green indicate positive and negative deviations, respectively. Dark zones indicate values of the indices equal or close to zero. Violet indicates that data were not available.

relative standard deviation are due to the passage of solar terminator in the sense described above, a very meticulous analysis was performed to verify whether each peak hour "fell" inside the hourly intervals delimiting the sunrise and sunset hours (Table 3). From this investigation emerges that only in a few cases, and for LSA, the observed peaks can be directly linked to the passage of solar terminator: at Rome, in August at sunset (18:00 UT, see Figures 4, 5, and 7), and

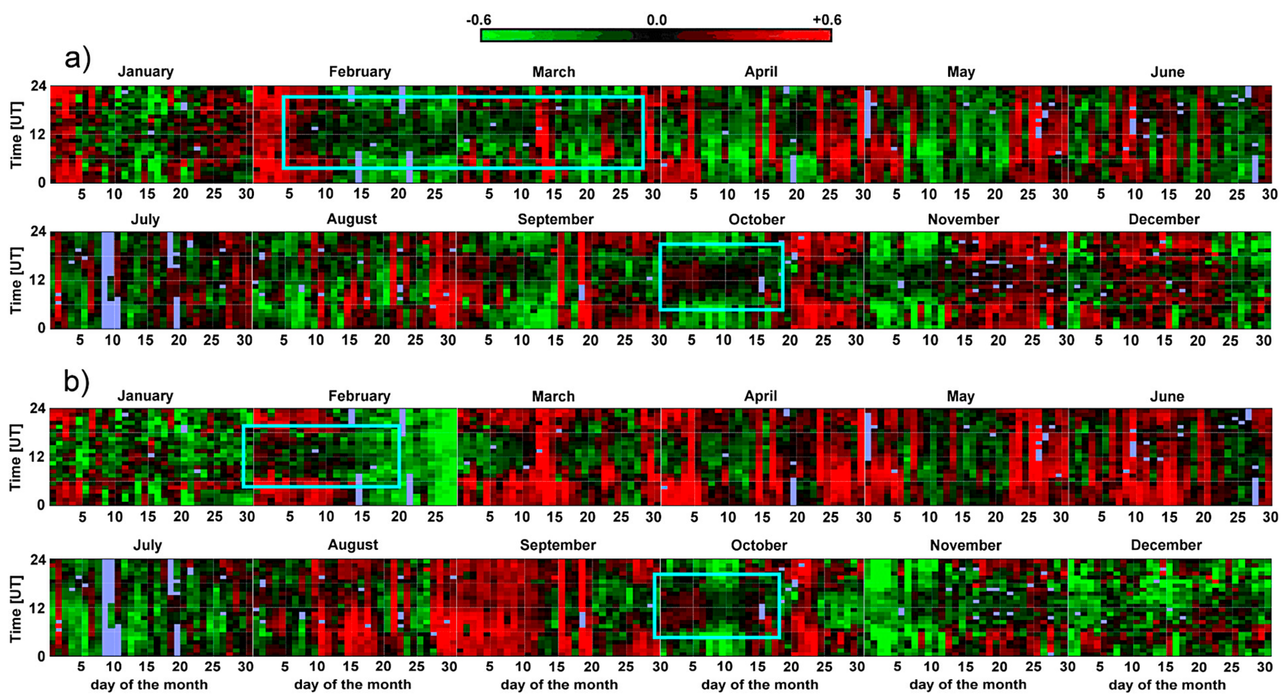

Figure 10. Same as Figure 9 but for HSA (year 1989). Light blue rectangles highlight zones where ionospheric variability is very low.

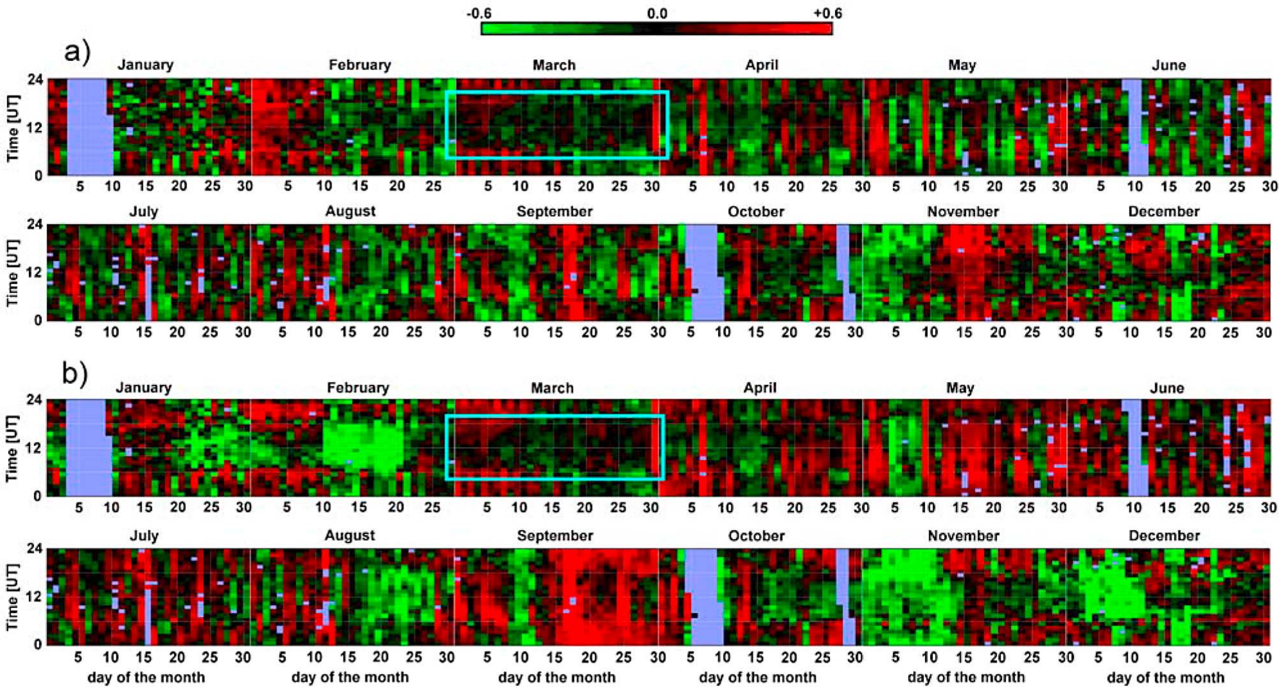

Figure 11. Same as Figure 10 but for year 2000.

November again at sunset (16:00 UT, see Figures 4 and 5); at Gibilmanna, in February at sunrise (06:00 UT, see Figures 4 and 5), and November at sunset (16:00 UT, see Figures 4, 5, and 7). This feature agrees with other studies [e.g., *Bilitza et al.*, 2004; *Akala et al.*, 2010], which have shown the presence of peaks at sunrise and sunset clearly emerging from the diurnal trend.

[40] A more accurate investigation about the hours which are inside the sunrise/sunset sector (see Table 3), shows that in Rome, for HSA, ionospheric variability at these hours can

Table 3. Hours of Sunrise and Sunset for Rome and Gibilmanna[a]

Year 2011	Sunrise (UT)	Sunset (UT)	Daytime f_oF_2 Measurements (UT)	Nighttime f_oF_2 Measurements (UT)
			Rome	
Jan	06:38–06:24	15:49–16:22	16:00 (19)	16:00 (12)[b]
Feb	06:23–05:48	16:24–16:58	06:00 (9)	06:00 (19)[b]
Mar	05:46–04:56	16:59–17:33	05:00 (3), 17:00 (30)	05:00 (28), 17:00 (1)
Apr	04:54–04:09	17:34–18:06	18:00 (7)	18:00 (23)[b]
May	04:07–03:38	18:07–18:37	04:00 (25)	04:00 (6)[b]
Jun	03:38–03:38	18:38–18:49		
Jul	03:38–04:02	18:49–18:31	04:00 (29)	04:00 (2)
Aug	04:03–04:34	18:30–17:47	18:00 (22)	18:00 (9)[b]
Sep	04:35–05:05	17:46–16:56	05:00 (25), 17:00 (27)	05:00 (5), 17:00 (3)
Oct	05:06–05:40	16:54–16:07		
Nov	05:42–06:16	16:06–15:41	06:00 (16), 16:00 (6)	06:00 (14), [b]16:00 (24)[b]
Dec	06:17–06:38	1540–15:48		
			Gibilmanna	
Jan	06:23–06:13	15:57–16:28	16:00 (26)	16:00 (5)
Feb	06:12–05:41	16:29–16:58	06:00 (16)	06:00 (12)[b]
Mar	05:46–04:54	16:59–17:28	05:00 (3), 17:00 (30)	05:00 (28), 17:00 (1)
Apr	04:52–04:12	17:29–17:56		
May	04:11–03:46	17:57–18:23	04:00 (21), 18:00 (27)	04:00 (10),[b] 18:00 (4)
Jun	03:45–03:47	18:24–18:34		
Jul	03:47–04:08	18:34–18:17	04:00 (22)	04:00 (9)[b]
Aug	04:09–04:35	18:16–17:38	18:00 (15)	18:00 (16)[b]
Sep	04:36–05:01	17:37–16:52	05:00 (28), 17:00 (24)	05:00 (2), 17:00 (6)[b]
Oct	05:02–05:31	16:50–16:09		
Nov	05:32–06:03	16:08–15:47	06:00 (26), 16:00 (8)	06:00 (4), 16:00 (22)[b]
Dec	06:04–06:23	15:47–15:56		

[a]Second and third columns show the time intervals defining the hours of sunrise and sunset for Rome and Gibilmanna. Fourth and fifth columns specify the hours which "fall" inside the sunrise or sunset zone. Shown in parentheses are the number of times in which f_oF_2 measurements occur during nighttime and daytime for the considered month.

[b]Cases for which solar terminator is expected to affect mostly the ionospheric variability.

be, however, considered relatively high and therefore imputable to the passage of solar terminator, at sunrise for the months of February and May and at sunset for the months of January, April, August, and November. For LSA in Rome, the passage of solar terminator affects significantly ionospheric variability at sunset for the months of January, April, August, and November (for these two last months a peak of variability is also observed). At Gibilmanna the ionospheric variability is appreciably influenced by the solar terminator at sunset for the months of August, September, and November (where a peak of variability is also observed). These results confirm that relatively high values of ionospheric variability are observed actually in almost all cases (see footnoted entries in Table 3) for which the passage of solar terminator is expected to influence significantly ionospheric variability. At Rome, for June, October, and December, and at Gibilmanna, for April, June, October, and December, ionospheric variability is not imputable to solar terminator because f_oF_2 measurements do not occur during the passage of solar terminator but they are acquired always or before/after sunrise or before/after sunset. It is worth noting that for these months, in the transition from night to day, ionospheric variability described with the relative standard deviation, shows a more sharp decrease for LSA. From a careful comparison between Figures 4 and 7, it comes out that for many cases the variability peaks do not clearly emerge from the diurnal trends depicted in Figure 4. This because absolute standard deviation is used instead of normalized standard deviation [*Bilitza et al.*, 2004; *Akala et al.*, 2010], which has the effect of highlighting day-to-night differences. In fact, when the relative standard deviation is employed several variability peaks, especially before sunrise, and not observed with the absolute standard deviation, are highlighted for almost all months. Moreover, some maximums observed with the absolute standard deviation, but not with the relative standard deviation, occur mainly in the post sunset hours and in a larger extent for LSA. In particular, for LSA, the relative standard deviation better highlights the variability peaks already observed with the absolute standard deviation.

[41] As shown by Figure 6, on a monthly basis, f_oF_2 variability described by (3) and (4) shows a well defined *pseudo-wave* pattern. This pattern is in general less evident when the variability on a monthly basis is described by equation (6), nevertheless, comparing Figure 6a with Figure 8a, a very similar trend is observed from June to October with a sharp maximum in September that is better highlighted using equation (6) (see Figure 8a). Moreover, a peak in May and in September can be observed comparing Figure 6c and Figure 8c. At Gibilmanna the comparison between Figure 6e and Figure 8e shows a very similar trend from June to October with a sharp maximum in May that again emerges more clearly using equation (6). Although the behavior of ionospheric variability on a monthly basis shows some important common features when it is investigated by equations (3), (4), and (6), the dispersion indices (3) and (4) seem to be more effective in emphasizing a *pseudo-wave* pattern. In particular, when the dispersion indices (3) and (4) are used a semi-annual variation is clearly observed, with maximums occurring in the equinoctial months, this being more pronounced for HSA and by taking the index (2) into account (see Figure 6b). These results confirm those of *Rishbeth and Mendillo* [2001] who, by analyzing N_mF_2 variability at different midlatitude stations by means of absolute standard deviation, discovered a semi-annual variability with pronounced daytime equinoctial peaks. The semi-annual variation characterizing the f_oF_2 variability observed at Rome and Gibilmanna could be correlated with the semi-annual geomagnetic activity pattern discussed by *Joselyn* [1995]. In particular, the appearance of maximums during the equinoctial months could be explained considering that, on average, enhancements of the interplanetary magnetic field's southward component connecting to the geomagnetic field occur mainly near the equinoxes [*Russell and McPherron*, 1973].

[42] From a different perspective, these equinoctial peaks are explained as the effect of the coupling between the interplanetary magnetic field and the geomagnetic field being less effective at the solstices [*Cliver et al.*, 2000].

[43] The maps represented in Figures 9–11 show as the dispersion indices defined by equations (7) and (8) differ throughout the 24 h for each day of a given month. Violet sectors indicate that data were not available, red and green sectors indicate respectively positive and negative values of the indices, which means an ionospheric variability higher and lower than the mean level; dark sectors indicate that the variability with respect to the mean level is nearly null and therefore they point out the epochs in which the ionospheric plasma can be considered quiet.

[44] Analyzing carefully the contours diagrams shown in Figures 9–11, it can be seen that there is an evident difference between those obtained for LSA and those obtained for HSA. For LSA, the contour diagrams calculated according to the two delta indices (7) and (8) are reasonably similar and do not show any significant pattern. On the contrary, for HSA it emerges that at some epochs the two delta indices (7) and (8) depict f_oF_2 variability in a very different way, as it is evident for September 1989 in Figure 10a and Figure 10b. On the other hand, at other epochs, the two indices provide a very similar description of f_oF_2 variability. Moreover, from the HSA contour diagrams shown in Figure 10 and Figure 11, it can happen that around the equinoxes (see February, March, and October 1989 in Figure 10, and March 2000 in Figure 11), a relatively long sequence of days is characterized by a quiet ionosphere during the daytime (the dark zones highlighted by light blue rectangles in Figure 10 and Figure 11) and by marked variability during postsunset and nighttime hours. Even though these features need to be more deeply investigated, two mechanisms have been proposed. According to the first [e.g., *Laštovička*, 2006, and reference therein], the nighttime variability is due to upward propagating gravity waves (GWs), whose period ranges from tens of minutes to a few hours, from the lower atmosphere to the E and F ionospheric regions. Another explanation suggests that there are GWs of auroral origin, as there is a direct relationship between a source in the auroral zone and a wave observed at midlatitudes [*Williams et al.*, 1988]. This explanation is also supported by the work of many authors who observed a correlation between nighttime GWs and high values of the magnetic activity index K_p ($K_p > 3$) [e.g., *MacDougall et al.*, 2009]. Besides these mechanisms, the main in situ source of GWs is the transition of solar terminator [*Somsikov*, 1995]. The rapid increase/decrease of solar radiation at sunrise/sunset can act as a source of

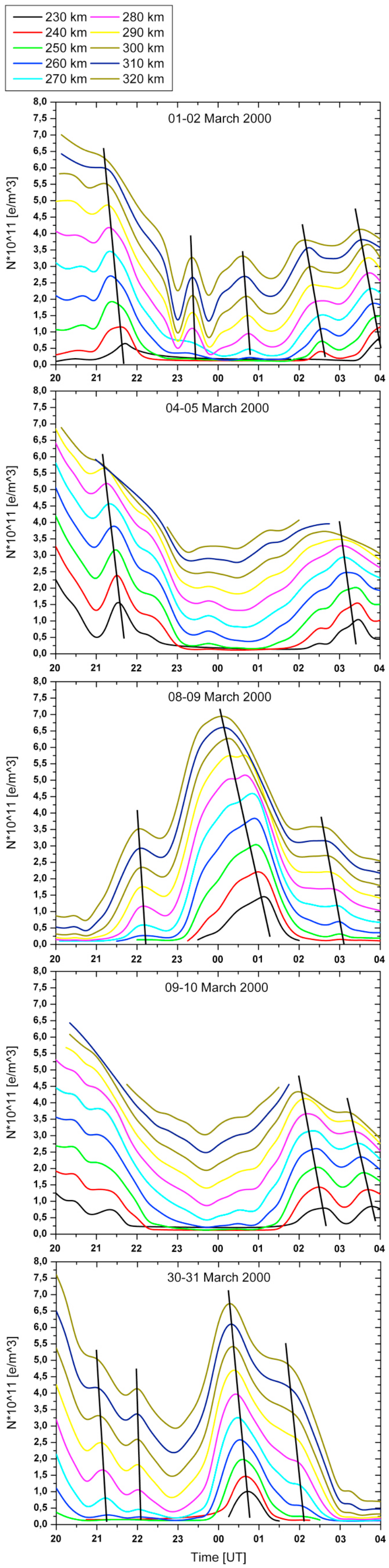

Figure 12. Electron density variations for the real height range 230–320 km computed for 5 days of March 2000 from 20:00 to 04:00 UT. Oblique line highlights the downward phase shift typical of gravity wave propagation.

atmospheric irregularities and generate GWs in the F region [*Somsikov and Ganguly*, 1995], although the evening terminator transition excites less regular and weaker GW effects [*Altadill et al.*, 2004]. By analyzing rapid sequences of ionosonde measurements, the signature of GW propagation in the F region was also inferred during nighttime by *Boška and Laštovicka* [1996]. Moreover, GW signatures were also found in the lower ionosphere by analyzing nighttime measurements of low frequency radio wave absorption [*Lastovicka et al.*, 1993]. Therefore, in the light of these studies, the variability of f_oF_2 observed during postsunset nighttime hours in the equinoctial months of February, March, and October 1989, and March 2000, could be explained in terms of overlapping GWs of auroral origin and GWs propagating from the lower atmosphere to the upper ionosphere, triggered by the sunset solar terminator. In order to highlight more clearly the gravity wave pattern behavior, a further analysis was performed taking into account the nighttime ionograms recorded in March 2000 by the Digisonde [*Bibl and Reinisch*, 1978] installed at Rome. From these ionograms, the vertical electron density profiles given as output by Automatic Real-Time Ionogram Scaler With True Height analysis (ARTIST) [*Reinisch and Huang*, 1983] were analyzed. From the profiles (N, h), where N is the electron density and h is the real height of reflection, isoheight curves $N(h = \text{const} = 230, 240, 250, 260, 270, 280, 290, 300, 310, 320$ km) were calculated. Figure 12 shows that isoheight curves relative to five nights of March 2000, that are included in the blue rectangles marked in Figure 11, present maximum N variations occurring first at 320 km and then at lower heights, showing a downward phase shift which is characteristic of GW propagation at the typical heights of the ionospheric F1 and F2 layers [*Hines*, 1960]. Therefore these results demonstrate the presence of traveling ionospheric disturbances (TIDs) caused by gravity wave (GW) propagation, and support the hypothesis of GWs propagating from the lower atmosphere assumed on the basis of the results shown in Figures 9–11.

5. Summary

[45] This paper described a preliminary study of f_oF_2 variability over Rome and Gibilmanna, Italy, for LSA and HSA. In order to perform the analysis, two different kinds of f_oF_2 data sets, and different dispersion indices were considered to highlight diverse aspects characterizing ionospheric variability. Both absolute and relative standard deviation, as well as the dispersion index based on the quiet time reference values of f_oF_2, put in evidence a greater ionospheric variability for HSA at Rome limitedly to certain hours: 00:00–02:00 UT and 20:00–23:00 UT in winter months, 00:00–10:00 UT in equinoctial months, and 04:00–16:00 UT in summer months. The absolute and relative standard deviation results, analyzed around midday (09:00–13:00 UT), provide essentially the same following outcomes: at Rome ionospheric variability is

smaller in case of LSA during summer months; at Gibilmanna ionospheric variability is greater than that in Rome during winter and summer months, and a little smaller during equinoctial months. Moreover, always around midday, for LSA, the f_oF_2 variability is smaller at the equinoxes than at the solstices, while for HSA, it is greater at equinoxes than at solstices. Again, from absolute and relative standard deviation, as well as from the dispersion index based on the quiet time reference values of f_oF_2, it was deduced that for LSA, at Gibilmanna the f_oF_2 variability is in general larger than at Rome, especially in summer, and characterized by a number of relative minimums and maximums greater than those observed at Rome. Therefore, it can be argued that Gibilmanna, especially in summer, is more inclined to variability, with its lower latitude resulting in an ionosphere affected by more numerous dynamic processes. Maximums of variability clearly in connection with the passage of solar terminator at sunset, are observed for LSA at Rome in August (18:00 UT) and November (16:00 UT). Also in Gibilmanna clear variability peaks directly linked to the passage of solar terminator at sunrise/sunset are observed in February (06:00 UT) and November (16:00 UT) respectively. Furthermore, relatively high values of variability are observed at those hours for which the passage of solar terminator is expected to influence significantly ionospheric variability. The relative standard deviation seems to be more effective than absolute standard deviation in highlighting the variability peaks observed before sunrise, but less efficient in emphasizing the *pseudo-wave* pattern and consequently the semi annual variation observed when the ionospheric variability is analyzed on a monthly basis. On the other side, the absolute standard deviation is able to highlight some maximums (not observed with relative standard deviation) mostly in the post sunset hours. The abrupt changes of f_oF_2 variability from daytime to nighttime conditions observed for HSA in some days of the equinoctial months seem to be related to upward propagating gravity waves triggered by solar terminator.

[46] On the whole, the results obtained agree with those of previous studies. However, some peculiar features emerged, the causes of which are not altogether clear. With the aim of estimating the relative solar, geomagnetic, and meteorological contribution to F2-layer variability, further studies considering quiet and disturbed geomagnetic conditions separately are planned. Besides providing a better understanding of ionospheric variability, these studies could be helpful for developing a corresponding statistical model, which would be valuable when scheduling frequencies for HF services.

[47] **Acknowledgments.** Robert Lysak thanks the reviewers for their assistance in evaluating this paper.

References

Akala, A. O., A. B. Adeloye, and E. O. Somoye (2010), Ionospheric f_oF_2 variability over the Southeast Asian sector, *J. Geophys. Res.*, *115*, A09329, doi:10.1029/2010JA015250.
Altadill, D., E. M. Apostolov, J. Boska, and P. Sauli (2004), Planetary and gravity wave signatures in the F region ionosphere with impact to radio propagation predictions and variability, *Ann. Geophys.*, *47*(2–3), 1109–1119.
Bibl, K., and B. W. Reinisch (1978), The universal digital ionosonde, *Radio Sci.*, *13*, 519–530, doi:10.1029/RS013i003p00519.
Bilitza, D., O. K. Obrou, J. O. Adeniyi, and O. Oladipo (2004), Variability of *fo*F2 in the equatorial ionosphere, *Adv. Space Res.*, *34*(9), 1901–1906, doi:10.1016/j.asr.2004.08.004.
Boška, J., and J. Laštovicka (1996), Gravity wave activity in the lower ionosphere and in the F2 region—Similarities and differences, *Adv. Space Res.*, *18*(3), 127–130, doi:10.1016/0273-1177(95)00851-5.
Buonsanto, M. J. (1999), Ionospheric storms—A review, *Space Sci. Rev.*, *88*, 563–601, doi:10.1023/A:1005107532631.
Cander, L. R., and S. J. Mihajlovic (1998), Forecasting ionospheric structure during the great geomagnetic storms, *J. Geophys. Res.*, *103*(A1), 391–398, doi:10.1029/97JA02418.
Chen, Y., and L. Liu (2010), Further study on the solar activity variation of daytime N_mF_2, *J. Geophys. Res.*, *115*, A12337, doi:10.1029/2010JA015847.
Cliver, E. W., Y. Kamide, and A. G. Ling (2000), Mountains versus valleys: Semiannual variation of geomagnetic activity, *J. Geophys. Res.*, *105*, 2413–2424, doi:10.1029/1999JA900439.
David, M., and J. J. Sojka (2010), Single-day dayside density enhancements over Europe: A survey of a half-century of ionosonde data, *J. Geophys. Res.*, *115*, A12311, doi:10.1029/2010JA015711.
Davis, R. M., and N. L. Groome (1964), Variations of the 3000 km MUF in time and space, *NBS Rep. 8498*, U.S. Dep. of Commer., Washington, D. C.
Elias, A. G. (2009), Trends in the F2 ionospheric layer due to long-term variations in the Earth's magnetic field, *J. Atmos. Sol. Terr. Phys.*, *71*(14–15), 1602–1609, doi:10.1016/j.jastp.2009.05.014.
Ezquer, R. G., M. Mosert, R. Corbella, M. Erazù, S. M. Radicella, M. Cabrera, and L. de la Zerda (2004), Day-to-day variability of ionospheric characteristics in the American sector, *Adv. Space Res.*, *34*(9), 1887–1893, doi:10.1016/j.asr.2004.03.016.
Forbes, M. J., E. S. Paolo, and X. Zhang (2000), Variability of the ionosphere, *J. Atmos. Sol. Terr. Phys.*, *62*(8), 685–693, doi:10.1016/S1364-6826(00)00029-8.
Fotiadis, D. N., G. M. Baziakos, and S. S. Kouris (2004), On the global behaviour of the day-to-day MUF variation, *Adv. Space Res.*, *33*(6), 893–901, doi:10.1016/j.asr.2003.05.005.
Fox, M. W., and P. J. Wilkinson (1988), A study of OWF conversion factors in the Australian region, *Tech. Rep., IPS-TR-88–02*, 28 pp., IPS Radio and Space Serv., Sydney, N. S. W., Australia.
Fuller-Rowell, T. J., M. V. Codrescu, R. G. Roble, and A. D. Richmond (1997), How does the thermosphere and ionosphere react to a geomagnetic storm?, in *Magnetic Storms*, *Geophys. Monogr. Ser.*, vol. 98, edited by B. T. Tsurutani et al., pp. 203–225, AGU, Washington D. C., doi:10.1029/GM098p0203.
Hines, C. O. (1960), Internal atmospheric gravity waves at ionospheric heights, *Can. J. Phys.*, *38*, 1441–1481, doi:10.1139/p60-150.
International Telecommunication Union (ITU) (1997), *HF Propagation Prediction Method Recommendation*, 533 pp., Geneva.
Jarvis, M. J. (2009), Longitudinal variation in E- and *F* region ionospheric trends, *J. Atmos. Sol. Terr. Phys.*, *71*(13), 1415–1429, doi:10.1016/j.jastp.2008.05.017.
Joselyn, J. A. (1995), Geomagnetic activity forecasting: State of the art, *Rev. Geophys.*, *33*, 383–401, doi:10.1029/95RG01304.
Kazimirovsky, E. S. (2002), Coupling from below as a source of ionospheric variability: A review, *Ann. Geophys.*, *45*(1), 1–29.
Kouris, S. S., D. N. Fotiadis, and T. D. Xenos (1998), On the day to day variation of *fo*F2 and M(3000)F2, *Adv. Space Res.*, *22*(6), 873–876, doi:10.1016/S0273-1177(98)00116-1.
Kouris, S. S., D. N. Fotiadis, and B. Zolesi (1999), Specifications of the F-region variations for quiet and disturbed CONDITIONS, *Phys. Chem. Earth*, *24*(4), 321–327, doi:10.1016/S1464-1917(99)00005-7.
Kozin, I. D., V. I. Kozin, and I. N. Fedulina (1995), On a choice of the ionospheric disturbance indices, *Geomagn. Aeron.*, *35*(1), 111–112.
Laštovička, J. (2006), Forcing of the ionosphere by waves from below, *J. Atmos. Sol. Terr. Phys.*, *68*(3–5), 479–497, doi:10.1016/j.jastp.2005.01.018.
Lastovicka, J., J. Boska, and D. Buresova (1993), Digital measurements of LF radio wave absorption in the lower ionosphere and inferred gravity wave activity, *Ann. Geophys.*, *11*, 937–946.
Liu, L., M. He, X. Yue, B. Ning, and W. Wan (2010), Ionosphere around equinoxes during low solar activity, *J. Geophys. Res.*, *115*, A09307, doi:10.1029/2010JA015318.
Liu, L., Y. Chen, H. Le, V. I. Kurkin, N. M. Polekh, and C.-C. Lee (2011), The ionosphere under extremely prolonged low solar activity, *J. Geophys. Res.*, *116*, A04320, doi:10.1029/2010JA016296.
MacDougall, J. W., G. Li, and P. T. Jayachandran (2009), Traveling ionospheric disturbances near London, Canada, *J. Atmos. Sol. Terr. Phys.*, *71*(17–18), 2077–2084, doi:10.1016/j.jastp.2009.09.016.
Pietrella, M., and L. Perrone (2008), A local ionospheric model for forecasting the critical frequency of the F2 layer during disturbed geomagnetic and ionospheric conditions, *Ann. Geophys.*, *26*(2), 323–334, doi:10.5194/angeo-26-323-2008.

Prolss, G. W. (1995), Ionospheric F region storms, in *Handbook of Atmospheric Electrodynamics*, vol. 2, edited by H. Volland, pp. 195–248, CRC Press, Boca Raton, Fla.

Prölss, G. W. (1997), Magnetic storm associated perturbations of the upper atmosphere, in *Magnetic Storms*, *Geophys. Monogr. Ser.*, vol. 98, edited by B. T. Tsurutani et al., pp. 227–241, AGU, Washington D. C., doi:10.1029/GM098p0227.

Reinisch, B. W., and X. Huang (1983), Automatic calculation of electron density profiles from digital ionograms: 3. Processing of bottom side ionograms, *Radio Sci.*, *18*(3), 477–492, doi:10.1029/RS018i003p00477.

Rishbeth, H. (1993), Day-to-day ionospheric variations in a period of high solar activity, *J. Atmos. Terr. Phys.*, *55*(2), 165–171, doi:10.1016/0021-9169(93)90121-E.

Rishbeth, H., and M. Mendillo (2001), Patterns of F2-layer variability, *J. Atmos. Sol. Terr. Phys.*, *63*(15), 1661–1680, doi:10.1016/S1364-6826(01)00036-0.

Rishbeth, H., M. Mendillo, J. Wroten, and R. G. Roble (2009), Day-by-day modelling of the ionospheric F2-layer for year 2002, *J. Atmos. Sol. Terr. Phys.*, *71*(8–9), 848–856, doi:10.1016/j.jastp.2009.03.022.

Romano, V., S. Pau, M. Pezzopane, E. Zuccheretti, B. Zolesi, G. De Franceschi, and S. Locatelli (2008), The electronic Space Weather upper atmosphere (eSWua) project at INGV: Advancements and state of the art, *Ann. Geophys.*, *26*, 345–351, doi:10.5194/angeo-26-345-2008.

Rush, C. M., and J. Gibbs (1973), Predicting the day-to-day variability of the mid-latitude ionosphere for application to HF propagation predictions, *Rep. TR-73–0335*, Cambridge Res. Lab., Air Force Geophys. Lab., Hanscom Air Force Base, Mass.

Russell, C. T., and R. L. McPherron (1973), Semiannual variation of geomagnetic activity, *J. Geophys. Res.*, *78*, 92–108, doi:10.1029/JA078i001p00092.

Somoye, E. O., A. O. Akala, and A. Ogwala (2011), Day to day variability of h′F and *fo*F2 during some solar cycle epochs, *J. Atmos. Sol. Terr. Phys.*, *73*(13), 1915–1922, doi:10.1016/j.jastp.2011.05.004.

Somsikov, V. M. (1995), On the mechanism for the formation of atmospheric irregularities in the solar terminator region, *J. Atmos. Terr. Phys.*, *57*(1), 75–83, doi:10.1016/0021-9169(93)E0017-4.

Somsikov, V. M., and B. Ganguly (1995), On the formation of atmospheric inhomogeneities in the solar terminator region, *J. Atmos. Terr. Phys.*, *57*(12), 1513–1523, doi:10.1016/0021-9169(95)00014-S.

Triskova, L., V. Truhlik, and K. Podolska (2011), Time delays in the correlation between solar activity and the F2 region plasma frequency, *J. Atmos. Sol. Terr. Phys.*, *73*(5), 623–626, doi:10.1016/j.jastp. 2010.12.017.

Wakai, N., H. Ohyama, and T. Koizumi (1987), *Manual of Ionogram Scaling*, 3rd version, Radio Res. Lab., Minist. of Posts and Telecommun., Tokyo.

Wilkinson, P. J. (2004), Ionospheric variability and the international reference ionosphere, *Adv. Space Res.*, *34*(9), 1853–1859, doi:10.1016/j.asr.2004.08.007.

Williams, P. J. S., et al. (1988), The generation and propagation of atmospheric gravity waves observed during the Worldwide Atmospheric Gravity-wave Study (WAGS), *J. Atmos. Terr. Phys.*, *50*(4–5), 323–338, doi:10.1016/0021-9169(88)90018-9.

Wrenn, G. L., A. S. Rodger, and H. Rishbeth (1987), Geomagnetic storms in Antarctic *F* region: I. Diurnal and seasonal patterns in main phase effects, *J. Atmos. Terr. Phys.*, *49*(9), 901–913, doi:10.1016/0021-9169(87)90004-3.

Zolotukhina, N., N. Polekh, and O. Pirog (2011), Variability of the ionosphere over Irkutsk at low solar activity, *Adv. Space Res.*, *48*(10), 1606–1612, doi:10.1016/j.asr.2011.08.006.